

Time and Frequency Domain Response of HTS Resonators for Use as NMR Transmit Coils

Ghoncheh Amouzandeh , *Student Member, IEEE*, Vijaykumar Ramaswamy, Nicolas Freytag, Arthur S. Edison , Lawrence A Hornak , *Senior Member, IEEE*, and William W. Brey 

Abstract—Replacing normal metal NMR coils with thin-film high-temperature superconductor (HTS) resonators can significantly improve the sensitivity of analytical NMR. To study the use of these resonators for excitation as well as detection, we investigated the radio frequency properties of the HTS NMR coils in both frequency and time domain at a variety of transmit power levels. Experiments were conducted on a double-sided, counter wound spiral resonator designed to detect NMR signals from ^{13}C nuclei at 14.1 T. Power-dependent nonlinearity was observed in the transmission coefficient and quality factor. The ability of the HTS resonators to accurately generate short pulses was studied in the time domain over the range power levels. The results of this study show that some form of Q switching is needed to get good transmit performance from HTS coils for ^{13}C . For that purpose, the effect of adding a shorted transmission line stub to improve the pulse shapes and reduce phase transients was studied.

Index Terms—Nuclear magnetic resonance, high-temperature superconductors, superconducting devices.

I. INTRODUCTION

NUCLEAR Magnetic Resonance (NMR) is a powerful technique to study the structure of metabolites and proteins in chemistry and biology. NMR signals arise from the small nuclear magnetization that many isotopes such as ^1H and ^{13}C develop parallel to a strong magnetic field. Although ^1H is most commonly observed, detecting ^{13}C can provide more direct information about backbone structure of biological molecules as they are primarily made of carbon scaffolds [1]. The role of an NMR transmit coil is to produce radio-frequency (RF) pulses to tip the magnetization away from the direction of the magnetic field. The magnetization then precesses at the Larmor frequency

which can be detected as a small RF voltage in a pick-up coil. The resulting signal is termed the free induction decay (FID). Because the Larmor frequency is shifted slightly due to the local electronic environment, different chemical sites within a molecule can be identified and form an informative spectrum. This effect is known as “chemical shift”. To excite the whole chemical shift range uniformly and effectively requires both strong and short ($10\ \mu\text{s}$ – $20\ \mu\text{s}$) RF pulses. Detecting the FID also requires a short dead time between the end of the RF pulse and beginning of the acquisition during which the current in the transmit coil is allowed to decay.

Replacing normal metal NMR coils with thin-film high-temperature superconducting (HTS) coils in cryogenically cooled NMR probes can significantly improve the sensitivity and signal-to-noise ratio (SNR) due to the high quality (Q) factor of superconducting resonators [2]–[7]. The improved sensitivity is especially helpful for direct ^{13}C detection due to its low gyromagnetic ratio and 1% natural abundance. By using HTS coils in probes optimized for ^{13}C detection, metabolomics information of compounds with as little material as 40 nmols can be studied [1].

The high Q factors of HTS resonators provide higher sensitivity in reception and also higher efficiency in transmission. However, the same high Q factor will reduce the system bandwidth for both reception and excitation. For nuclides such as ^1H with a narrow (~ 12 ppm) chemical shift range, the reduction in bandwidth is not problematic. However, ^{13}C has a much wider chemical shift range of approximately 200 ppm which makes the use of high Q resonators challenging. Additionally, when the current density in the HTS resonator is large enough to effectively excite NMR magnetization, RF dissipation increases which has been reported to result in pulse shape distortions, flip angle misalignment and coil-transmitter mismatch in NMR and MRI coils [8]–[11]. Power handling and the nonlinear response of the HTS thin films under strong RF signals has been also investigated in other areas such as filters [12], [13], and metamaterials [14], [15]. For the use of HTS thin film resonators for NMR transceive applications it is important to investigate the effect of high Q factor and current compression on RF pulse shape and amplitude. Long pulse ring-down time can significantly increase the NMR dead time.

In this project, the RF properties of an HTS thin film resonator designed to be used as a ^{13}C NMR transceive coil were investigated. The results, especially with non-linearity, may vary significantly between devices, so the measurements presented

Manuscript received November 1, 2018; accepted February 26, 2019. Date of publication March 4, 2019; date of current version April 29, 2019. This work was supported in part by NIH/NIGMS under Grants R01GM120151 and P41 GM122698 and in part by Bruker Biospin. A portion of the work was done at the National High Magnetic Field Laboratory, which is supported in part by the NSF through Cooperative Agreements DMR-1157490 and DMR-1644779, and in part by the State of Florida. (*Corresponding author: William W. Brey.*)

G. Amouzandeh is with the National High Magnetic Laboratory and the Department of Physics, Florida State University, Tallahassee, FL 32310 USA (e-mail: ga13d@my.fsu.edu).

W. W. Brey is with the National High Magnetic Laboratory, Florida State University, Tallahassee, FL 32310 USA (e-mail: wbrey@magnet.fsu.edu).

V. Ramaswamy and N. Freytag are with Bruker Biospin AG, Faellanden 8117, Switzerland (e-mail: vijaykumar.ramaswamy@bruker.com; nicolas.freytag@bruker.com).

A. S. Edison and L. A. Hornak are with the University of Georgia, Athens, GA 30602 USA (e-mail: aedison@uga.edu; lahornak@uga.edu).

Color versions of one or more of the figures in this paper are available online at <http://ieeexplore.ieee.org>.

Digital Object Identifier 10.1109/TASC.2019.2902522

here should be considered only as a single example. The double-sided, counter-wound spiral design is very similar to that was used in our ^{13}C -optimized NMR probe that was previously reported [1]. This design has several important advantages as a ^{13}C transceive coil. There is no difficulty to achieve the required 150 MHz resonance with the dimensions needed for an NMR transducer. The counterwound structure traps electric field within the substrate, away from the sample, reducing both loss and noise. Due to doubling the current carrying ability of a single sided design, it is possible to double the excitation field and reduce the excitation pulse length by 50%. The amplitude and phase response of the resonator was characterized using both frequency and time domain techniques. The duration and strength of pulses used in the time domain measurements were close to those used in practical NMR experiments and should represent the performance of the coil as it would be used by a biochemist in an NMR spectrometer. Finally, a simple method to reduce the rise and fall time of the resonator was tested.

II. MATERIAL AND METHOD

All experiments were conducted on a counter-wound spiral resonator with self-resonance of 139 MHz [16]. The device was patterned from a ~ 300 nm-thick film of $\text{Y}_1\text{Ba}_2\text{Cu}_3\text{O}_{7-\delta}$ (YBCO) covered with 120 nm *in situ* gold and coated on each side of the $432 \mu\text{m}$ -thick substrate of R-plane sapphire. The HTS wafer as described was supplied by Ceraco GmbH, Ismaning, Germany. The HTS rectangular resonant structure consisted of five turns of a $180 \mu\text{m}$ -wide trace. The trace was divided into seven parallel lines to reduce distortion of the NMR static polarizing field. In order to eliminate the additional modes, a 180 nm-thick gold layer was added as described in [17] to bridge the separate lines. The gold overlayer also reduces the quality factor, which was measured to be 4800 at 0 dBm in a single loop, power matched configuration. The overall length and width of the resonator is 20×3 mm. Star Cryoelectronics, USA, patterned and diced the wafer and added the patterned gold over layer as described above.

RF tests were performed using a closed-cycle helium Gifford-McMahon refrigeration system connected to a vacuum test chamber which is adapted to accommodate up to 5 sets of coils at a time for cryogenic testing. The test chamber has penetrations for RF connections and bellows which allow for adjustment of the position of inductive coupling loops. The coil under test was mounted on a cold head in the test chamber and enclosed by a cylindrical RF shield in the same manner as in previously reported NMR probes. For the tests reported here, the coil was cooled to approximately 30 K, well below the YBCO superconducting transition temperature (>87 K). Two movable normal metal loops were inductively coupled to the HTS coil. The first loop was adjusted to minimize the reflection coefficient under 0 dBm incident power at coil's resonance frequency. A second loop used as a pick-up was positioned so that the transmission coefficient S_{21} at resonance was below -22 dB. The S_{21} between the two loops above the transition temperature was -60 dB. We conducted RF tests in both frequency and time domain.

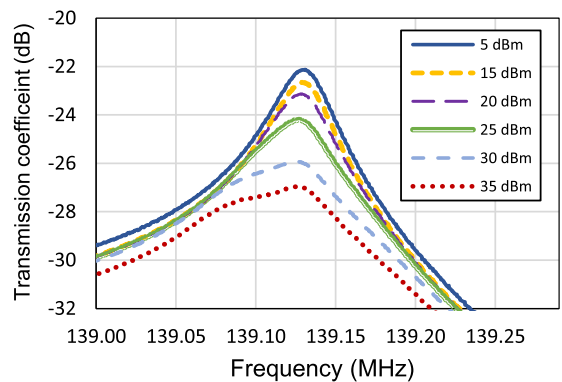


Fig. 1. Transmission plots at different power levels. Higher powers shift the resonance frequency down.

III. RESULT AND DISCUSSION

A. Frequency Domain Measurements

A vector network analyzer (VNA) was used to measure the HTS NMR coil response in the continuous wave (CW) mode to power levels from -10 to 20 dBm. To characterize the behavior of the coil under power levels above the normal limits of the VNA, a gate, pulse generator and power amplifier were also added. The gate reduced the duty cycle to 4% to avoid heating the resonators during the measurement. As NMR experiments are typically carried out with very low ($<1\%$) transmit duty cycle, this is appropriate for our tests as well. With the input bandwidth of the VNA set to minimum (15 Hz), and the VNA sweep triggered on the gate, noise that the gate would otherwise induce in the transmission measurement was minimized.

Fig. 1 shows the transmission plot of the coil for different pulse powers. Up to 5 dBm the coil Q (loaded by the drive loop and measured at -3 dB points) is around 4800. At higher power levels the peak broadens and is distorted. The increased loss in the resonator leads to a reduced transmission coefficient. To quantify the response of the HTS coil at high powers a framework was established to calculate the current in the coil from reflection and transmission measurements at each power level relative to the current at 0 dBm. The 0 dBm current was calculated from estimated inductance, resistance and the Q of the coil. The incident power was then increased, and the transmission and reflection parameters were measured for several power levels. Next, the gate, pulse generator and power amplifier were added to increase the available power to the levels of an NMR experiment. Some of the measurements in the pulsed mode that overlapped with the CW mode were used to calibrate the pulsed curve.

Fig. 2 shows that the coil was able to achieve a current of about 10.9 A at 35 dBm, a current at which we predict the 90° NMR transmit pulse would be $18 \mu\text{s}$ and the average current density to be about 3.28 MA/cm^2 . As Fig. 2 shows, above 15 dBm the coil response deviates significantly from linearity which was also observed in the transmission plots presented in Fig. 1. To linearize the current in the coil for NMR applications, it is possible to compensate with lookup tables. There could be an advantage of the compression at higher power, since the Q

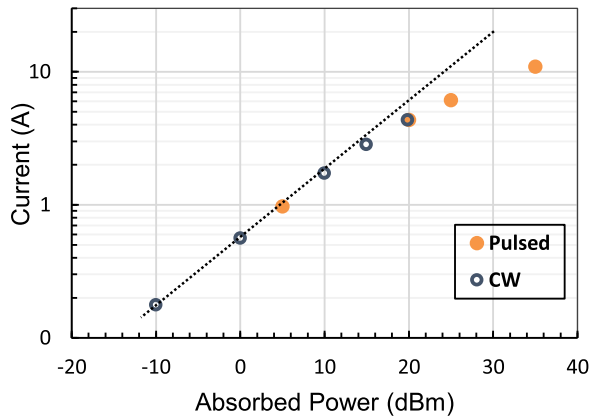


Fig. 2. Current in the HTS coil (log scale) as a function of absorbed power for the combination of pulsed and CW measurements.

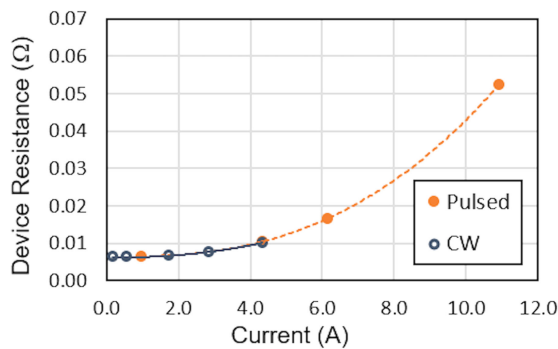


Fig. 3. Coil resistance expressed as a function of the current in the coil.

would drop which can provide a shorter dead time. For each power level of the experiment described above, the resistance of the HTS coil was calculated in addition to the current.

Fig. 3 shows the plot of the resistance versus the current in the coil. The *in situ* gold and the gold overlayer set a floor for the device resistance at low current. Above 4 A, the resistance increases with a power law exponent of about 2.5. Other studies have attributed the increase in dissipation to Joule heating [18] or weak links and other types of film defects [11], [14].

To characterize the nonlinearity in the HTS coil without driving the coil to full power, we measured second and third order harmonics as a function of input level with a spectrum analyzer. We employed a single tone rather than the more common two-tone test. We verified that changing the input level produced the expected slopes of 2 and 3 for the 2nd and 3rd order harmonics as shown in Fig. 4. The coil under test had a third order intercept of 45 dBm. While this test does not demonstrate that a device can produce the required RF magnetic field to meet specifications, it does better allow for direct comparison between devices.

B. Time Domain Measurements

To measure the HTS coil response in the time domain to short rectangular RF pulses, we utilized a Redstone NMR spectrometer transceiver (Tecmag, Houston, TX, USA). The pick-up and drive loops were positioned identically to the frequency domain

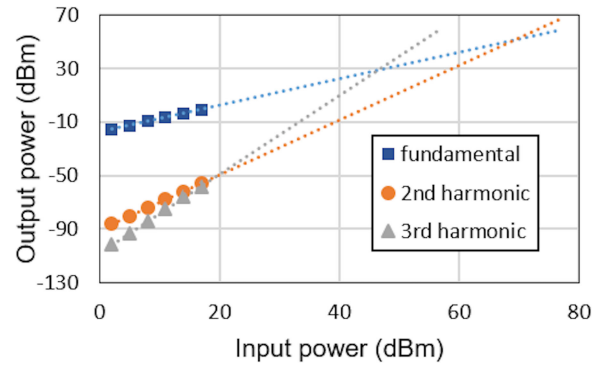


Fig. 4. Measured levels of the 2nd and 3rd order produced by a single input frequency have the expected slope and can be used to determine the intercept points.

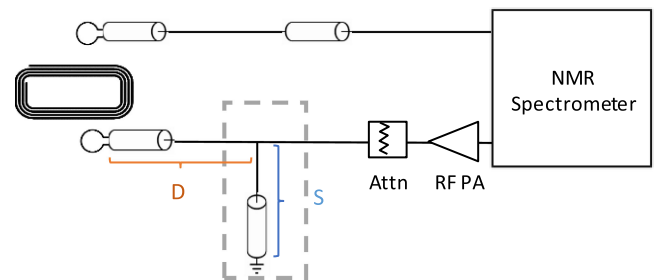


Fig. 5. Schematic of the experimental setup. Dotted region shows the shorted stub that was added later between the attenuator and the drive loop. RF PA refers to RF power amplifier.

measurements above. A 300 W RF power amplifier (AMT, Brea, CA, USA) followed by a 10 dB attenuator to ensure a consistent 50 Ω output was added between the spectrometer's transmit channel and the drive loop (Fig. 5).

A typical pulse to irradiate the entire ^{13}C band uniformly might be approximately 16 μs . We chose to drive our test coil with longer pulses in order to better characterize the rise and fall behavior. A series of 38 μs rectangular pulses at various power levels were applied to the drive loop at the resonance frequency of the coil. The pick-up loop was connected to the spectrometer's narrowband quadrature receiver allowing both the phase and magnitude components of the current in the HTS resonator to be recorded. The magnitude component of the received signals is shown in Fig. 6. For all power levels, the rise and fall times are long enough to affect the NMR transmit bandwidth. At the lowest incident power measured, 7 dBm, the resonator rings both up and down exponentially with a time constant (τ) of 11 μs . This corresponds to a loaded Q of about 4800 and is consistent with the low power frequency domain measurements. As the power increases, the rise time significantly improves, although the fall time was less sensitive. At the highest powers applied, 30 and 34 dBm, there is a small overshoot. It was possible to remove the overshoot by reducing the transmit frequency by about 6 Hz. We concluded that the overshoot may be due to a small tuning shift. Although we anticipated that HTS coils may decay faster at higher power due to their non-linearity and this may provide a shorter dead time, the pulse shapes at high

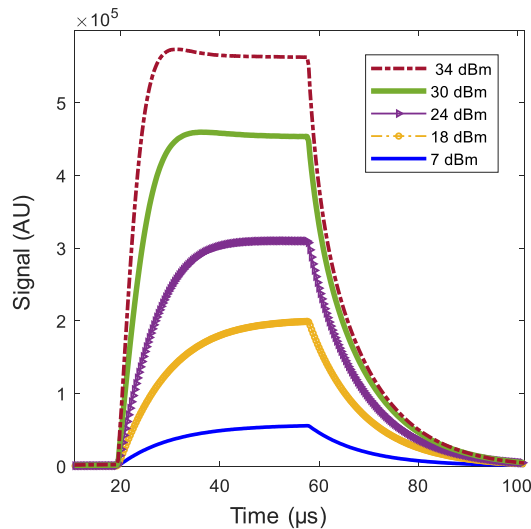


Fig. 6. Signal in the coil as a function of time for various powers. The coil was matched at low powers. AU stands for arbitrary unit.

power showed only a modestly shorter ring-down. The current in the coil at powers lower than 30 dBm decays exponentially with τ of approximately $11 \mu\text{s}$. However, at the highest power (34 dBm) the coil showed multi-exponential behavior. In the $5 \mu\text{s}$ after the end of the pulse, the signal decayed with an average τ of $7 \mu\text{s}$ but when the signal level was below 2.7×10^5 , started to ring down as a single exponential with τ of approximately $11 \mu\text{s}$.

To broaden the receive bandwidth to accommodate the full 200 ppm spectral dispersion of ^{13}C , we tried a simple approach of increasing the coupling to the point where the reflected power was 10 dB lower than the incident power. The effect of over-coupling on the sensitivity of the spectrometer will depend on the details of the low noise preamplifier, however for this modest amount of over-coupling we would not expect a large penalty. With over-coupling, the -3 dB bandwidth increased from approximately 28 kHz to 51 kHz or 340 ppm. Fig. 7a shows the pulse shapes under the same series of power levels for the over-coupled coil. At 7 dBm, τ was $\sim 6.25 \mu\text{s}$ compared to $11 \mu\text{s}$ with power matched coupling.

To further reduce the rise-up and ring-down time, we added a shorted stub, as shown in Fig. 5 to the circuit of the over-coupled coil. The stub reduces the circuit efficiency but improves transient response. In our test set up, the stub is present at all times during the acquisition. In an NMR spectrometer, the stub should be inserted between the RF power amplifier and the transmit-receive switch to take the stub out of the circuit during signal acquisition. Because the stub is not in the receive signal path, it will not reduce sensitivity.

For our test, we inserted a tee into the coaxial line between the RF power amplifier and the HTS resonator. We found that a stub length of 65 mm met the required transient response for ^{13}C NMR (S in Fig. 5). The stub and the transmission lines were RG-58 types. There was also a 10 dB power attenuator at the output of the RF power amplifier to absorb reflected power. Next, we varied the distance between the tee and the drive loop

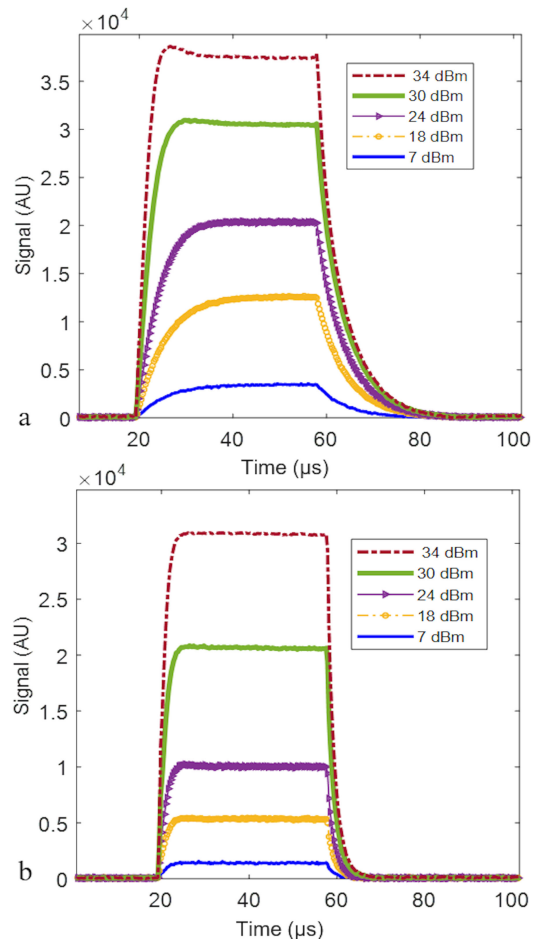


Fig. 7. Signal in the coil as a function of time for various powers. (a) Coil was over-coupled at low powers. (b) Coil was over-coupled and the shorted stub was also added.

by inserting M-M and F-F adapters (D in Fig. 5). We adjusted the number of adapters to maximize the -3 dB transmission bandwidth. The latter increased from 51 kHz to about 200 kHz, corresponding to a Q of 700. The pulse response of the modified system is shown in Fig. 7b, and the rise and fall time are both significantly improved. τ was reduced to $\sim 1.78 \mu\text{s}$ at 7 dBm. The efficiency was also noticeably reduced.

To compare the rise and fall numerically, the 10% to 90% time for rise-up and ring-down of power level 30 dBm from Fig. 7a is compared with power level 34 dBm from Fig. 7b. These two cases correspond to same current in the coil at signal level of 3×10^4 . Based on the result, rise-up and ring-down for 30 dBm were $6.1 \mu\text{s}$ and $12.6 \mu\text{s}$ while for 34 dBm of the stub added case they were respectively, $2.5 \mu\text{s}$ and $3.6 \mu\text{s}$, indicating significantly faster ring-up and ring-down with the addition of the shorted stub.

Another challenge inherent to use of high Q resonators for pulse transmission is the phase distortions they create at the beginning and end of an ideal pulse waveform. Ideally, the resonator would produce a magnetic field with a constant phase throughout the transmit pulse. A high-Q resonator produces a field with a transient deviation in the phase of the RF current

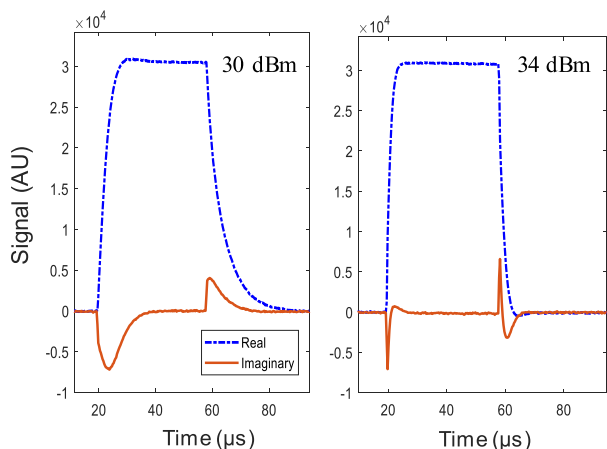


Fig. 8. Comparison of the in phase (blue-dot dash line) and quadrature (red) components of the signal in the coil without stub (left) at 30 dBm and with the stub (right) at 34 dBm.

during the ring up and ring down period. The effect of this phase error has been studied extensively in the NMR literature [19]–[23]. Fig. 8 shows both the in-phase (real) and quadrature (imaginary) components of the signal for the case without and with stub for power levels of 30 dBm and 34 dBm, respectively. The duration of the phase transient is significantly shortened with the stub.

IV. CONCLUSION

The properties of the HTS NMR resonators and the issues regarding their application as NMR transmitters for ^{13}C spectroscopy were investigated in this study. Although there was significant signal compression and a small shift in resonance frequency as power increased, it was possible to produce an RF magnetic field of sufficient strength for solution NMR experiments. Using the device with a low power matched Q factor of 5000, transient behavior may not be acceptable for NMR. However, modest over-coupling and inserting a passive stub were found to improve the transmit pulse shape and in particular reduce phase transients. For the future, these data will be combined with simulation studies to provide more insight into the nonlinear characteristics of the HTS NMR coils.

ACKNOWLEDGMENT

The authors would like to thank R. S. Withers for valuable input on the transmission shorted stub. S. Ranner, J. Kitchen, and I. Litvak are acknowledged for technical support.

REFERENCES

- [1] V. Ramaswamy, J. W. Hooker, R. S. Withers, R. E. Nast, W. W. Brey, and A. S. Edison, "Development of a ^{13}C -optimized 1.5-mm high temperature superconducting NMR probe," *J. Magn. Reson.*, vol. 235, pp. 58–65, Oct. 2013.
- [2] H. D. W. Hill, "Improved sensitivity of NMR spectroscopy probes by use of high-temperature superconductive detection coils," *IEEE Trans. Appl. Supercond.*, vol. 7, no. 2, pp. 3750–3755, Jun. 1997.

- [3] W. A. Anderson *et al.*, "High-sensitivity NMR spectroscopy probe using superconductive coils," *Bull. Magn. Reson.*, vol. 17, pp. 98–102, 1995.
- [4] W. W. Brey, A. S. Edison, R. E. Nast, J. R. Rocca, S. Saha, and R. S. Withers, "Design, construction, and validation of a 1-mm triple-resonance high-temperature-superconducting probe for NMR," *J. Magn. Reson.*, vol. 179, no. 2, pp. 290–293, Apr. 2006.
- [5] V. Ramaswamy, J. W. Hooker, R. S. Withers, R. E. Nast, A. S. Edison, and W. W. Brey, "Microsample cryogenic probes: Technology and applications," *eMagRes*, vol. 2, pp. 215–228, Mar. 2013.
- [6] S. Oikawa *et al.*, "Evaluation of superconducting pickup coil with high Q for 700 MHz NMR," *Proc. J. Phys.: Conf. Ser.*, vol. 507, 2014.
- [7] T. Yamada *et al.*, "Electromagnetic evaluation of HTS RF coils for nuclear magnetic resonance," *IEEE Trans. Appl. Supercond.*, vol. 25, no. 3, Jun. 2015, Art. no. 1500504.
- [8] S. E. Hurlston, W. W. Brey, S. A. Suddarth, G. A. Johnson, and E. G. Fitzsimons, "A high-temperature superconducting Helmholtz probe for microscopy at 9.4 T," *Magn. Reson. Med.*, vol. 41, no. 5, pp. 1032–1038, May 1999.
- [9] R. D. Black, T. A. Early, and G. A. Johnson, "Performance of a High-Temperature superconducting resonator for high-field imaging," *J. Magn. Reson. Ser. A*, vol. 113, no. 1, pp. 74–80, 1995.
- [10] A. S. Hall, N. M. Alford, T. W. Button, D. J. Gilderdale, K. A. Gehring, and I. R. Young, "Use of high temperature superconductor in a receiver coil for magnetic resonance imaging," *Magn. Reson. Med.*, vol. 20, no. 2, pp. 340–343, Aug. 1991.
- [11] O. Girard, J. C. Ginefri, M. Poirier-Quinot, and L. Darrasse, "Method for nonlinear characterization of radio frequency coils made of high temperature superconducting material in view of magnetic resonance imaging applications," *Rev. Sci. Instrum.*, vol. 78, no. 12, 2007.
- [12] R. R. Mansour, B. Jolley, S. Ye, F. S. Thomson, and V. Dokas, "On the power handling capability of high temperature superconductive filters," *IEEE Trans. Microw. Theory Techn.*, vol. 44, no. 7, pp. 1322–1338, Jul. 1996.
- [13] D. E. Oates, P. P. Nguyen, G. Dresselhaus, M. S. Dresselhaus, G. Koren, and E. Polturak, "Nonlinear surface impedance of YBCO thin films: Measurements, modeling, and effects in devices," *J. Supercond.*, vol. 8, no. 6, pp. 725–733, Dec. 1995.
- [14] C. Kurter, A. P. Zhuravel, J. Abrahams, C. L. Bennett, A. V. Ustinov, and S. M. Anlage, "Superconducting RF metamaterials made with magnetically active planar spirals," *IEEE Trans. Appl. Supercond.*, vol. 21, no. 3, pp. 709–712, Jun. 2011.
- [15] A. P. Zhuravel, C. Kurter, A. V. Ustinov, and S. M. Anlage, "Unconventional rf photoresponse from a superconducting spiral resonator," *Phys. Rev. B*, vol. 85, no. 13, p. 134535, Apr. 2012.
- [16] R. S. Withers, R. E. Nast, and W. A. Anderson, "NMR spiral RF probe coil pair with low external electric field," U.S. Patent 7 701 217, Apr. 2010.
- [17] V. Ramaswamy, J. W. Hooker, R. S. Withers, R. E. Nast, A. S. Edison, and W. W. Brey, "Development of a ^1H - ^{13}C dual-optimized NMR probe based on double-tuned high temperature superconducting resonators," *IEEE Trans. Appl. Supercond.*, vol. 26, no. 3, Apr. 2016, Art. no. 1500305.
- [18] J. Wosik, L. M. Xie, J. Mazierska, and R. Grabovickic, "Influence of columnar defects on surface resistance of $\text{YBa}_2\text{Cu}_3\text{O}_x$ superconducting thin films; Nonlinear effects," *Appl. Phys. Lett.*, vol. 75, no. 12, pp. 1781–1783, 1999.
- [19] T. M. Barbara, J. F. Martin, and J. G. Wurl, "Phase transients in NMR probe circuits," *J. Magn. Reson.*, vol. 93, no. 3, pp. 497–508, Jul. 1991.
- [20] M. Mehring and J. S. Waugh, "Phase transients in pulsed NMR spectrometers," *Rev. Sci. Instrum.*, vol. 43, no. 4, pp. 649–653, 1972.
- [21] Y. Tabuchi, M. Negoro, K. Takeda, and M. Kitagawa, "Total compensation of pulse transients inside a resonator," *J. Magn. Reson.*, vol. 204, no. 2, pp. 327–332, Jun. 2010.
- [22] J. Weber, M. Seemann, and J. Schmedt auf der Gönne, "Pulse-transient adapted C-symmetry pulse sequences," *Solid State Nucl. Magn. Reson.*, vol. 43–44, pp. 42–50, May 2012.
- [23] J. J. Wittmann, V. Mertens, K. Takeda, B. H. Meier, and M. Ernst, "Quantification and compensation of the influence of pulse transients on symmetry-based recoupling sequences," *J. Magn. Reson.*, vol. 263, pp. 7–18, Feb. 2016.